Tianjin Daxue Xuebao (Ziran Kexue yu Gongcheng Jishu Ban)/
Journal of Tianjin University Science and Technology
ISSN (Online):0493-2137
E-Publication: Online Open Access
Vol: 59 Issue: 06:2026
DOI: 10.5281/zenodo.20606131

CLINICAL AND RADIOGRAPHIC EVALUATION OF THREE DIMENSIONAL CUSTOMIZED TITANIUM MESH IN DEFICIENT POSTERIOR MANDIBULAR ALVEOLAR RIDGE AUGMENTATION

NOURHAN AHMED HUSSIEN*

Department of Oral and Maxillofacial Surgery, Faculty of Dentistry, MSA University, 6th October City, Egypt.
*Corresponding Author Email: nourhanabdulghany95@gmail.com

SHEREEN WAGDY

Department of Oral and Maxillofacial Surgery, Faculty of Dentistry, MSA University, 6th October City, Egypt.

AHMED ELRAWDY

Department of Oral and Maxillofacial Radiology, Faculty of Dentistry, Suez Canal University, Ismailia, Egypt.

MOHAMED SAID HAMED

Department of Oral and Maxillofacial Surgery, Faculty of Dentistry, Suez Canal University, Ismailia, Egypt.

Abstract

Aim: This study aimed to clinically and radiographically evaluate the efficacy, predictability, and safety of combining a customized three-dimensional (3D) printed titanium mesh with a 'sticky bone' composite graft (particulate xenograft and Platelet-Rich Fibrin) for complex vertical and horizontal alveolar ridge augmentation in the posterior mandible, concurrent with dental implant placement. **Patients and Methods:** Eight systemically healthy patients (three males, five females, aged 34-65) presenting with severe atrophy of the posterior mandibular alveolar ridge were enrolled. A full digital workflow was employed, starting with Cone-Beam Computed Tomography (CBCT) to digitally plan the augmentation and design the patient-specific 3D titanium mesh. The surgical procedure involved full-thickness flap reflection, simultaneous placement of dental implants (n=16), stabilization of the customized mesh over the defect, and filling the space with a 'sticky bone' graft. Flap primary closure was achieved with tension-free suturing. Clinical assessment, post-operative pain (VAS), and radiographic evaluation (CBCT) for dimensional changes in height and width were performed over a 6-month period, after which the meshes were removed. **Results:** All surgical sites healed uneventfully, demonstrating a 100% implant and augmentation survival rate at 6 months. Postoperative radiographic analysis confirmed a highly significant increase in both dimensions: the mean alveolar ridge height increased by 47.1% ± 12.4% ($p < 0.001$), and the mean alveolar ridge width increased by 155.4% ± 62.1% ($p < 0.001$). The customized meshes exhibited excellent adaptation, with a mean deviation of only 0.3371 ± 0.1760 mm. Minimal, transient soft tissue dehiscence was observed in two cases, with no mesh exposure noted at the 6-month follow-up. **Conclusion:** The digital workflow utilizing a customized 3D titanium mesh in conjunction with a sticky bone graft is a highly effective, precise, and predictable technique for achieving significant vertical and horizontal augmentation of the severely atrophied posterior mandibular alveolar ridge, thereby ensuring a favorable and stable foundation for dental implant placement.

Keywords: 3D Titanium Mesh, Cone-Beam Computed Tomography, Bone Graft, Mandibular Alveolar Ridge Augmentation.

Tianjin Daxue Xuebao (Ziran Kexue yu Gongcheng Jishu Ban)/
Journal of Tianjin University Science and Technology
ISSN (Online):0493-2137
E-Publication: Online Open Access
Vol: 59 Issue: 06:2026
DOI: 10.5281/zenodo.20606131

INTRODUCTION

The predictable loss of alveolar bone height and width following tooth extraction poses a major challenge for prosthetic rehabilitation and implant therapy. Adequate alveolar bone volume and quality at the implant site are critical for long-term implant stability. To mitigate post-extraction resorption, clinicians employ strategies ranging from immediate implant placement and socket preservation to delayed ridge augmentation when significant deficiency exists. Within guided bone regeneration (GBR), bone grafting materials particularly xenografts such as deproteinized bovine bone (DBBB) are widely used because their architecture resembles human bone and provides an osteoconductive scaffold for new bone apposition.

Posterior mandibular defects with combined horizontal and vertical deficiencies are especially challenging. Conventional GBR with particulate grafts and resorbable or non-resorbable membranes can yield satisfactory results but may suffer from limitations including inadequate space maintenance, membrane exposure, and graft migration in larger defects. To address these issues, customized three-dimensional (3D) titanium meshes have been introduced. Additive manufacturing enables patient-specific meshes that precisely fit alveolar defects, improving space maintenance, graft stability, and angiogenesis while potentially reducing soft tissue complications compared with conventional membranes (Ciocca *et al*., 2011; Cucchi *et al*., 2020).

Alveolar resorption proceeds rapidly after tooth loss (Atwood *et al*., 1971) and can compromise denture retention, implant placement, nutrition, and quality of life (Sahyoun *et al*., 2003; Raghoebar *et al*., 2005). Mandibular resorption is particularly rapid approximately twice that of the maxilla (Tallgren *et al*., 1972) and is influenced by local (tooth loss, periodontitis) and systemic factors (e.g., diabetes) (Taylor *et al*., 1996). Various classification systems guide clinical decision-making, including Branemark's quantity/quality classes (1985), Cawood and Howell's six-stage alveolar resorption classification (1988), and the Juodzbalys and Raustia ridge atrophy types for implant planning (2004). Bone density classifications by Lekholm and Zarb (1985) and HU-based schemes (Misch and Kircos, 1999) further inform implant site assessment and predict insertion torque and primary stability (Trisi *et al*., 1999).

Reconstructive options for the atrophic posterior mandible include nerve repositioning, short implants, distraction osteogenesis, onlay and interpositional grafts, and GBR with membranes or titanium mesh. Each technique has distinct advantages and complication profiles; choice depends on defect characteristics and surgeon expertise (Chiapasco *et al*., 2009). Autogenous bone remains the gold standard due to osteogenic potential, but donor-site morbidity and resorption limit its use. Allografts and xenografts (notably bovine-derived products) offer availability and reduced morbidity, with xenografts demonstrating long-term residual particles and comparable implant survival in many studies (Del Fabbro *et al*., 2008). Membrane selection affects GBR outcomes. Collagen membranes are biocompatible but variably resorbable, whereas PTFE and titanium-reinforced PTFE provide durable barriers but risk infection if exposed. Titanium meshes meet many ideal membrane criteria rigidity for space maintenance, porosity for vascularization, and shape

Tianjin Daxue Xuebao (Ziran Kexue yu Gongcheng Jishu Ban)/
Journal of Tianjin University Science and Technology
ISSN (Online):0493-2137
E-Publication: Online Open Access
Vol: 59 Issue: 06:2026
DOI: 10.5281/zenodo.20606131

stability yet prefabricated meshes can be poorly adaptive and increase soft-tissue complications. Customized 3D-printed titanium meshes, fabricated from CBCT-derived stereolithographic models, improve fit, reduce operative time, standardize graft volume, and support vascularized regeneration while permitting optimization of thickness and pore size to balance mechanical strength and soft-tissue healing (Dolcini *et al*., 2016; Lizio *et al*., 2022; Di Spirito *et al*., 2024).

Adjuncts such as advanced platelet-rich fibrin (A-PRF) and “sticky bone” (PRF combined with particulate grafts) enhance soft-tissue healing, graft handling, and angiogenic/osteogenic signaling, further improving GBR predictability (Dohan Ehrenfest *et al*., 2009; Miron *et al*., 2017; Arafat *et al*., 2022). This study evaluates the clinical and radiographic efficacy of 3D-customized titanium meshes in augmenting deficient posterior mandibular ridges for subsequent implant placement. This study aimed to evaluate the 3D customized titanium mesh in deficient posterior mandibular alveolar ridge augmentation clinically and radiographically.

MATERIALS AND METHODS

Materials

1) 3D customized Ti-mesh: Medical Titanium grade 4 milled using a Millstar machine (Taiwan). Mesh surfaces were polished to promote soft-tissue healing and reduce flap dehiscence.
2) Titanium micro-screws and screwdriver: Titanium micro-screws (0.2 mm, Taiwan) and the screwdriver were supplied unsterilized and sterilized prior to use for apical fixation of the Ti-mesh.
3) Implants: Sixteen tapered dental implants (Neo Biotech, Korea) were placed in the posterior mandibular region simultaneously with the sticky bone and Ti-mesh. Implant diameters ranged from 3.5 to 4.5 mm and lengths from 8.5 to 10 mm.
4) Xenograft: OneXeno Graft (OGXBS10; 1.0 ml ≤ 2 mm cortico-cancellous bovine bone graft powder, Korea) supplied in sterile vials. Xenograft was hydrated with sterile saline and A-PRF on a sterilized dish before application. Vial volumes of 1.0 cc and 1.5 cc were used according to defect size.
5) Electric centrifuge: An 80-1 Desktop electric centrifuge (maximum 4000 rpm; capacity 6 × 20 ml) was used to prepare A-PRF from patient venous blood. Samples were centrifuged at 200 g for 8 minutes to separate red blood cells, an intermediate fibrin clot (PRF), and acellular plasma. The fibrin clot was retrieved, red blood cells removed, excess serum expressed on dry gauze, and the A-PRF clot incubated at room temperature for 10 minutes before use in sticky bone preparation.

Study design and setting

An in vivo randomized clinical trial conducted in two phases at the Oral and Maxillofacial Clinic, Faculty of Dentistry, Suez Canal University Hospital. Phase I comprised ridge augmentation with 3D customized Ti-mesh and simultaneous implant placement; phase

Tianjin Daxue Xuebao (Ziran Kexue yu Gongcheng Jishu Ban)/
Journal of Tianjin University Science and Technology
ISSN (Online):0493-2137
E-Publication: Online Open Access
Vol: 59 Issue: 06:2026
DOI: 10.5281/zenodo.20606131

II comprised Ti-mesh removal after 6 months. Eight Ti-meshes were placed in eight patients requiring implant placement in deficient posterior mandibular alveolar ridges. Each patient received two implants in the premolar–molar area (total 16 implants). Patients presented with vertical and horizontal ridge resorption; ages ranged 34–65 years; three males and five females.

Ethics and consent

The study purpose and procedures were explained to all participants and written informed consent was obtained according to guidelines of the Research Ethics Committee, Faculty of Dentistry, Suez Canal University.

Sample size calculation

Sample size was calculated according to Daniel (1999) and Charan and Biswas (2013) using the standard normal variate ($Z = 1.96$ at $P < 0.05$), the standard deviation of the variable (SD), and the desired absolute error or precision (d).

Eligibility criteria

Inclusion criteria: good oral hygiene; moderate to severe posterior mandibular bone resorption; residual bone height ≤ 5 mm; minimum bucco-lingual width 4 mm; medically free or controlled systemic conditions. Exclusion criteria: heavy smoking (>10 cigarettes/day); uncontrolled systemic disease; alcohol or drug abuse; acute or chronic head and neck infections; history of immunosuppressive therapy, chemotherapy, or radiotherapy within 5 years.

Preoperative management

Patient interview and clinical evaluation documented demographic data, medical/surgical/dental history, functional complaints, and postoperative expectations (Table 1). Clinical examination recorded oral hygiene, mucosal quality and pathology, occlusion, neighboring teeth condition, and inter-arch space. Professional debridement and oral hygiene instructions were provided one week before surgery. All patients received prophylactic antibiotic (2 g long-acting penicillin) one hour preoperatively.

Table 1: Demographic data of all patients included in the study

Patient Number	Implant Number	Age	Gender	Defective Bone site
1	2	65	Male	lower right posterior mandible
2	2	65	Male	lower left posterior mandible
3	2	53	Male	lower left posterior mandible
4	2	45	Female	lower right posterior mandible
5	2	34	Female	lower right posterior mandible
6	2	37	Female	lower left posterior mandible
7	2	40	Female	lower right posterior mandible
8	2	47	Female	lower left posterior mandible

Radiographic evaluation and virtual planning

Preoperative CBCT scans were obtained for all patients to measure available bone height and width and to exclude intra-osseous pathology. A SCANORA cone beam 3D scanner

Tianjin Daxue Xuebao (Ziran Kexue yu Gongcheng Jishu Ban)/
Journal of Tianjin University Science and Technology
ISSN (Online):0493-2137
E-Publication: Online Open Access
Vol: 59 Issue: 06:2026
DOI: 10.5281/zenodo.20606131

was used with FOV W 5 × 10 cm, 0.4 mm voxels, tube voltage 90 kVp, current 10 mA, and exposure 20 s. OnDemand3D software was used for dimensional assessment. Virtual implant planning and customized Ti-mesh design were performed with RealGuide software using DICOM files to respect neighboring teeth and the inferior alveolar canal and to determine desired contour for ridge augmentation (Fig. 1).

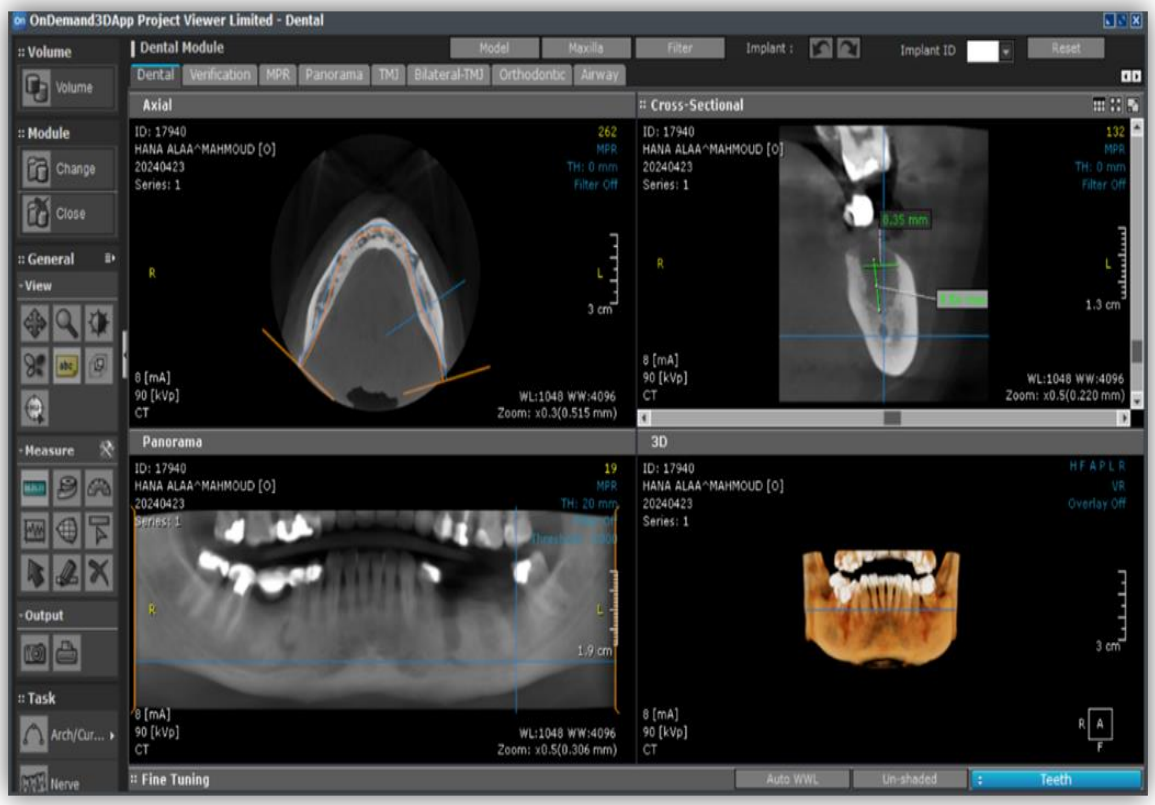

Figure 1: preoperative CBCT scan

SLA models and Ti-mesh manufacturing

Virtually augmented 3D mandible models were printed for each case (Fig. 2). Ti-mesh design followed implant-driven prosthetic planning and virtual comparison with the contralateral side to determine target bone levels. Bone segmentation and graft generation defined the desired contour; clinical applicability was checked virtually. Mini-screw holes (0.2 mm) were positioned apically; pores were distributed across the mesh body to promote pseudo-periosteal formation. Manufacturing (Di Spirito *et al*. 2024) used Medical Titanium grade 4 milled from CAD STL files and CAM programs on a Millstar machine. Post-milling steps included deburring, polishing rounded mesh borders to reduce soft tissue perforation, anodizing to generate an oxide layer, cleaning, and packing (Fig. 3).

Tianjin Daxue Xuebao (Ziran Kexue yu Gongcheng Jishu Ban)/
Journal of Tianjin University Science and Technology
ISSN (Online):0493-2137
E-Publication: Online Open Access
Vol: 59 Issue: 06:2026
DOI: 10.5281/zenodo.20606131

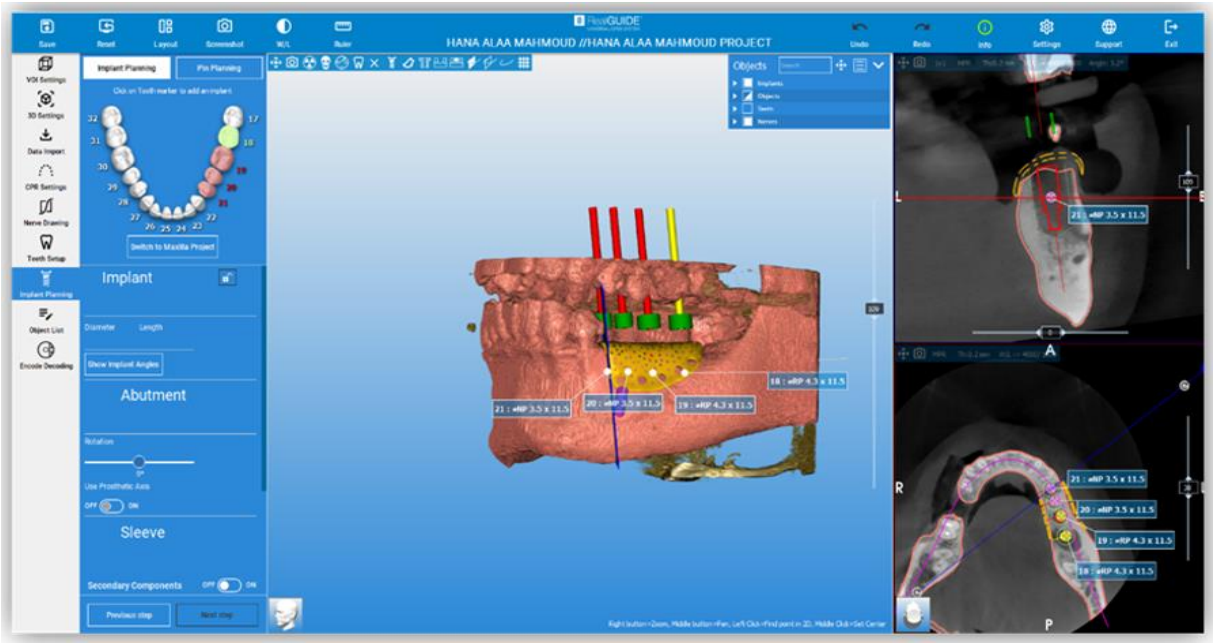

Figure 2: Ti mesh designed on RealGuide software

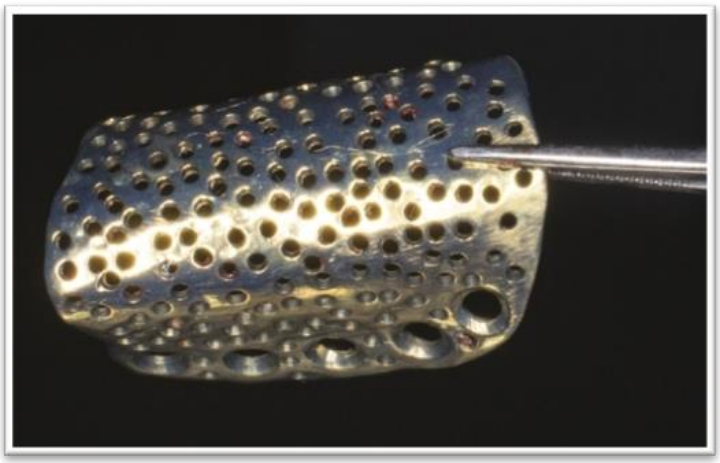

Figure 3: Image showing Ti mesh after polishing

Operative procedures

All procedures were performed under local anesthesia (Mepicaine HCL 2% with Levonordefrin 1:20,000). A labial para-crestal incision was made, preserving the mental nerve. A full-thickness mucoperiosteal flap exposed the ridge. The 3D Ti-mesh was tried in and adapted to the defect (Fig. 4 & 5). Implant osteotomies were drilled first and implants placed motor-driven according to the virtual plan (Fig. 6). Corticotomies were performed through the buccal and crestal cortical plates using a long-shank rose head carbide bur #2 at low speed with copious irrigation to enhance revascularization (Fig. 7).

Tianjin Daxue Xuebao (Ziran Kexue yu Gongcheng Jishu Ban)/
Journal of Tianjin University Science and Technology
ISSN (Online):0493-2137
E-Publication: Online Open Access
Vol: 59 Issue: 06:2026
DOI: 10.5281/zenodo.20606131

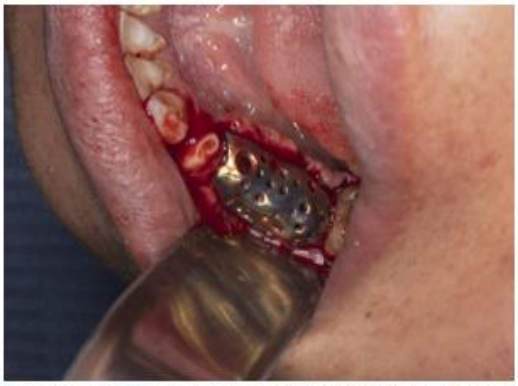

Figure 4: Clinical image showing Ti mesh try in

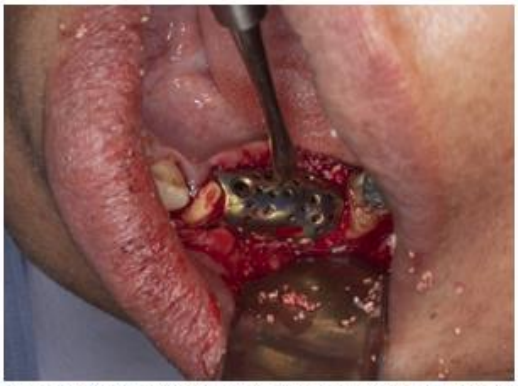

Figure 5: Clinical image showing Ti mesh try in

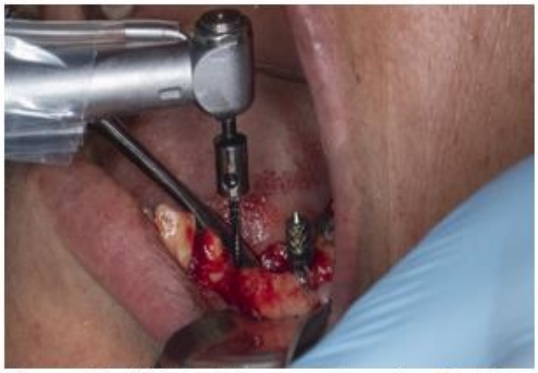

Figure 6: Clinical image showing Drilling osteotomies for implants

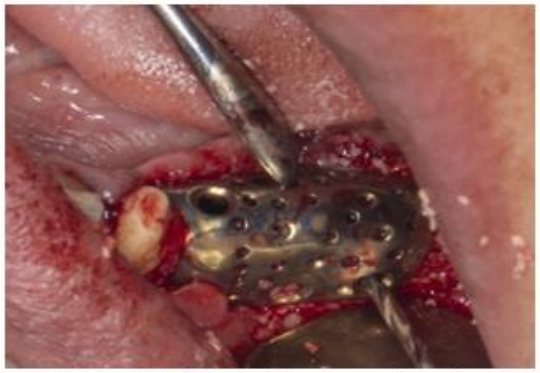

Figure 7: Clinical image showing corticotomies through the Ti mesh

A-PRF preparation and sticky bone

A-PRF was prepared from 20 ml autologous venous blood collected into two 10 ml tubes without anticoagulant and centrifuged on-table (protocol specified). The A-PRF clot was separated, red cell fractions discarded, and A-PRF placed on dry gauze to remove excess serum. Cancellous xenograft particles (0.25 mm) were mixed with A-PRF to produce sticky bone (Fig. 8).

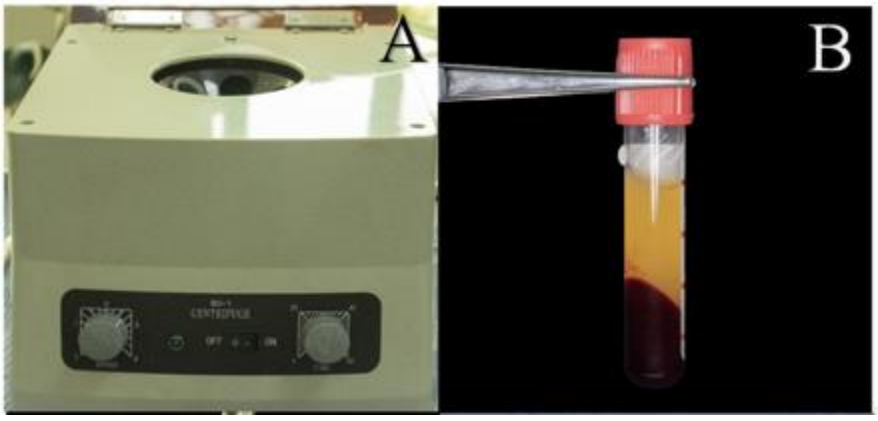

Tianjin Daxue Xuebao (Ziran Kexue yu Gongcheng Jishu Ban)/
Journal of Tianjin University Science and Technology
ISSN (Online):0493-2137
E-Publication: Online Open Access
Vol: 59 Issue: 06:2026
DOI: 10.5281/zenodo.20606131

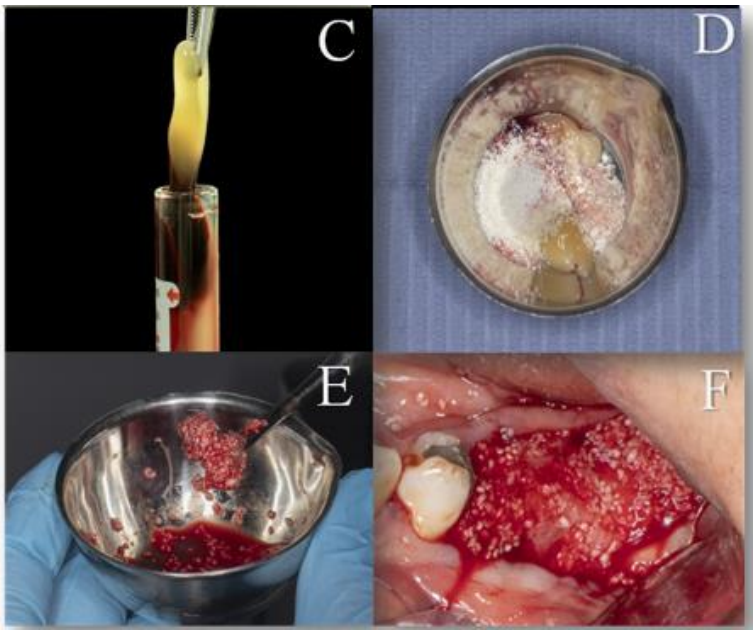

Figure 8: Steps of PRF & sticky bone preparation. A: Centrifuge, B:Test-tube with A-PRF, C: A-PRF extracted from tube, D:Bone graft with A-PRF, E:Sticky bone, F: Sticky bone adapted to alveolar ridge

Graft placement and fixation

Sticky bone was placed on the inner surface of the Ti-mesh and adapted to the deficient ridge; the assembly was inserted in the recipient site. Ti-mesh was fixated with micro-screws (0.2 mm), with at least two buccal and one crestal screw to ensure stability. Submucosal dissection and periosteal releasing incisions allowed tension-free water-tight closure with Vicryl 4-0 sutures (Fig. 9, Fig. 10).

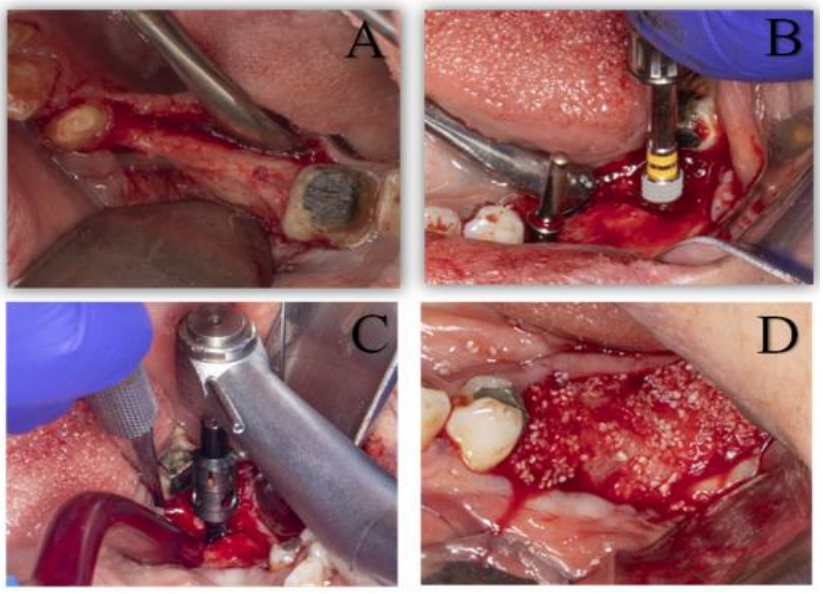

Tianjin Daxue Xuebao (Ziran Kexue yu Gongcheng Jishu Ban)/
Journal of Tianjin University Science and Technology
ISSN (Online):0493-2137
E-Publication: Online Open Access
Vol: 59 Issue: 06:2026
DOI: 10.5281/zenodo.20606131

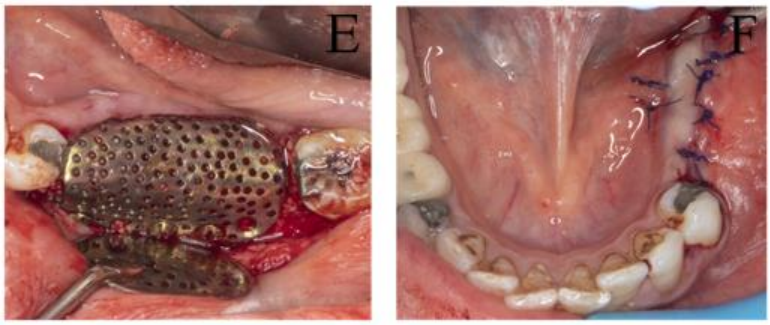

Figure 9: Case no 1. A: alveolar ridge after flap reflection, B: placing implants, C: Drilling of 2nd premolar implant, D: Bone graft adapted to alveolar ridge, E: Ti mesh screwed to the ridge, F: After suturing

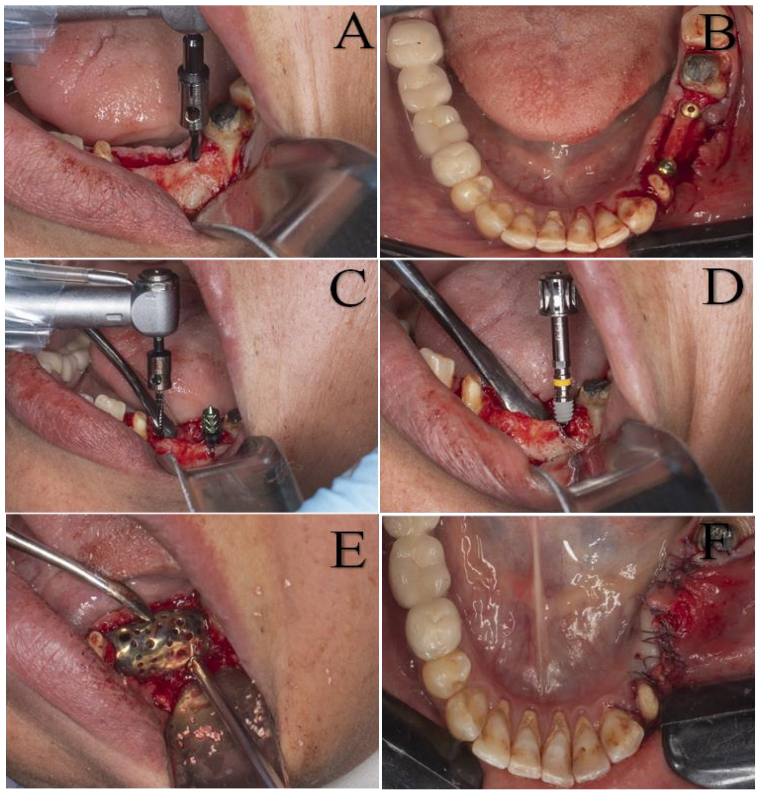

Figure 10: Case no 2. A: Ridge after flap exposure. B: Alveolar ridge after implants placement, C: drilling of implant, D: Implant placement, E: screwing of mesh into the ridge, F: Suturing

Postoperative care

Postoperative instructions were standardized: extra-oral cold application during the first day; Betadine 1% mouthwash three times daily starting day 2; Augmentin 1 g every 12 hours for one week; diclofenac sodium IM every 12 hours for three days then orally for

Tianjin Daxue Xuebao (Ziran Kexue yu Gongcheng Jishu Ban)/
Journal of Tianjin University Science and Technology
ISSN (Online):0493-2137
E-Publication: Online Open Access
Vol: 59 Issue: 06:2026
DOI: 10.5281/zenodo.20606131

three days; suture removal at 10 days; soft diet for one week; removable prostheses prohibited.

Outcome assessment and radiographic follow-up

At 6 months, CBCT (OnDemand3D) was repeated to assess vertical height and horizontal width (Fig. 13). Linear measurements at two points per augmented site (planned lower second premolar and second molar positions) were obtained from identical CBCT slices and imported into RealGuide software for evaluation of achieved vertical height (measured from 2 mm above the inferior alveolar nerve to the augmented crest) and horizontal width (buccal to lingual cortical distance at the crest) and for assessment of Ti-mesh positioning accuracy relative to the virtual design (Figures 11 & 12).

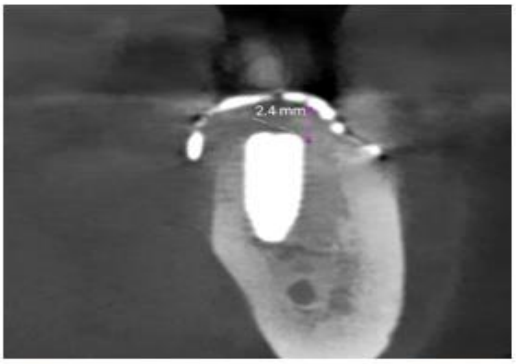

Figure 11: post-operative CBCT showing increase in width

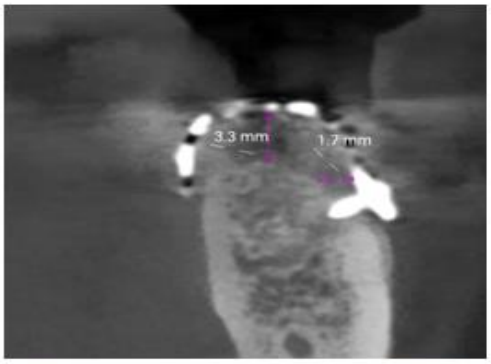

Figure 12: post-operative CBCT showing increase in height

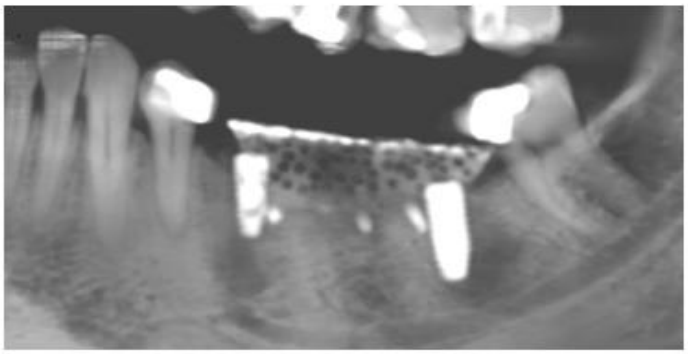

Figure 13: post-operative CBCT showing mesh in place

RESULTS

Surgical outcomes

The surgical procedures were generally well tolerated. All implants demonstrated improved healthy bone levels and intact soft tissues except for two cases that exhibited minimal soft tissue dehiscence at two weeks postoperatively. These instances of dehiscence were managed conservatively with chlorhexidine mouthwash three times daily for one week. By the end of the six-month follow-up period none of the cases showed

Tianjin Daxue Xuebao (Ziran Kexue yu Gongcheng Jishu Ban)/
Journal of Tianjin University Science and Technology
ISSN (Online):0493-2137
E-Publication: Online Open Access
Vol: 59 Issue: 06:2026
DOI: 10.5281/zenodo.20606131

mesh exposure or persistent soft tissue dehiscence. There were no clinical signs of mobility in the underlying implants and no failures of the bone augmentation procedure, yielding a six-month survival rate of 100%.

Statistical Analysis

Data were calculated, tabulated, and statistically analyzed. Continuous variables are presented as mean ± standard deviation (SD), median (Mdn), minimum and maximum. Data normality was assessed using the Shapiro–Wilk test. Descriptive statistics are reported as Mean ± SD. The Wilcoxon signed-rank test was used to compare visual analogue scale (VAS) scores. An alpha level of 0.05 was applied. Statistical analyses were performed using IBM SPSS (version 26, Armonk, USA). P values ≤ 0.05 were considered statistically significant. Statistical analysis was performed using SPSS for Windows version 26.0 (IBM Corp., Armonk, NY), with significance interpreted at P ≤ 0.05.

A. Bone Height

Postoperative assessment of augmented ridge bone height demonstrated a statistically significant increase when compared with preoperative measurements ($p < 0.001$). The mean ridge bone height increased from 8.7 ± 1.3 mm preoperatively to 12.6 ± 1.4 mm postoperatively. This corresponds to a mean percentage increase in bone height of 47.1 ± 12.4%. Bone height data are presented in Table 2 and illustrated in Fig. 14.

Table 2: Descriptive statistics of Bone height

	Bone height					p-value	% of change in bone height (mm)				
	Mean	SD	Mdn	Min	Max		Mean	SD	Mdn	Min	Max
pre-operative	8.7	1.3	8.6	6.3	11.6	<0.001	47.1	12.4	47.7	27.4	66.5
post-operative	12.6	1.4	12.4	10.5	15.5						

*significant, NS=non-significant

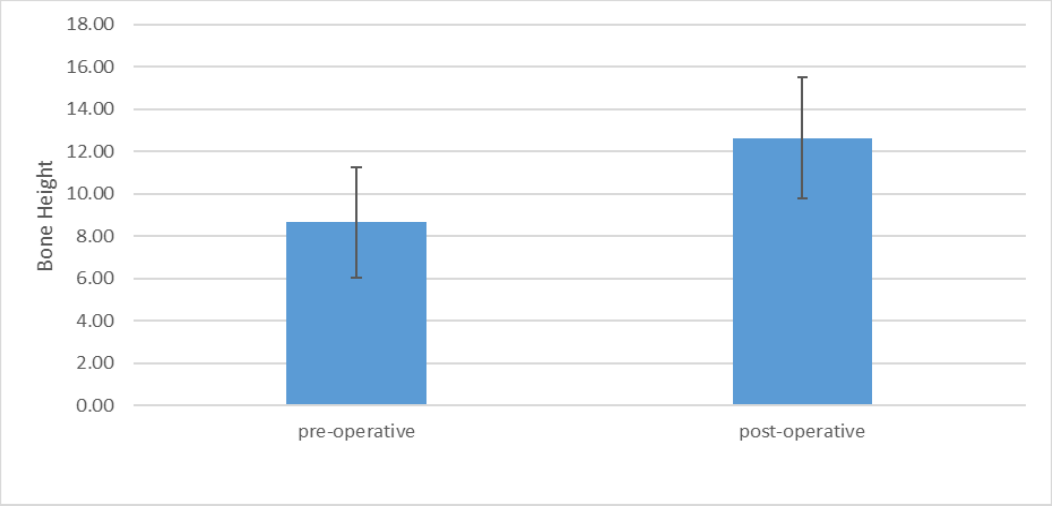

Figure 14: Bar chart showing the mean Bone Height

Tianjin Daxue Xuebao (Ziran Kexue yu Gongcheng Jishu Ban)/
Journal of Tianjin University Science and Technology
ISSN (Online):0493-2137
E-Publication: Online Open Access
Vol: 59 Issue: 06:2026
DOI: 10.5281/zenodo.20606131

B. Bone Width

Postoperative assessment of augmented ridge bone width also demonstrated a statistically significant increase compared with preoperative values ($p < 0.001$). The mean ridge bone width increased from 3.3 ± 0.8 mm preoperatively to 8.0 ± 0.8 mm postoperatively. The mean percentage increase in bone width was 155.4 ± 62.1%. Bone width data are presented in Table 3 and illustrated in Fig. 15.

Table 3: Descriptive statistics of Bone Width

	Bone width					p-value	% of change in bone width (mm)				
	Mean	SD	Mdn	Min	Max		Mean	SD	Mdn	Min	Max
pre-operative	3.3	0.8	3.2	2.0	5.1	<0.001	155.4	62.1	154.7	62.7	273.0
post-operative	8.0	0.8	8.1	6.5	9.2						

*significant, NS=non-significant

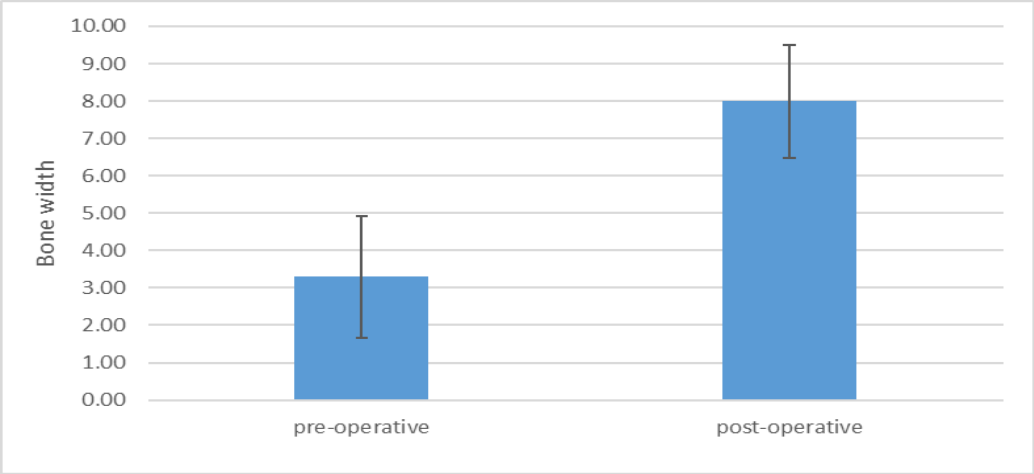

Figure 15: Bar chart showing the mean Bone Width

C. VAS Score

Analysis of postoperative pain using the VAS revealed a significant reduction in pain at day 7 compared with day 1 ($p < 0.001$). Although mean pain scores decreased by day 3, this intermediate reduction was not statistically significant when compared to day 1 ($p = 0.137$). Mean VAS pain scores were 7.1 ± 1.1 at day 1, 4.1 ± 1.1 at day 3, and 1.5 ± 1.3 at day 7. VAS data are summarized in Table 5 and depicted in Fig. 16.

Table 4: Descriptive statistics of VAS score data

	VAS					p-value
	Mean	SD	Mdn	Min	Max	
Day 1	7.1	1.1	7.0	6.0	9.0	<0.001
Day 3	4.1	1.1	4.0	3.0	6.0	
Day 7	1.5	1.3	1.5	0.0	4.0	

Different letter within Mean values indicates significant difference (Dunn Bonferroni Adjusted), *=significant, NS=non-significant

Tianjin Daxue Xuebao (Ziran Kexue yu Gongcheng Jishu Ban)/
Journal of Tianjin University Science and Technology
ISSN (Online):0493-2137
E-Publication: Online Open Access
Vol: 59 Issue: 06:2026
DOI: 10.5281/zenodo.20606131

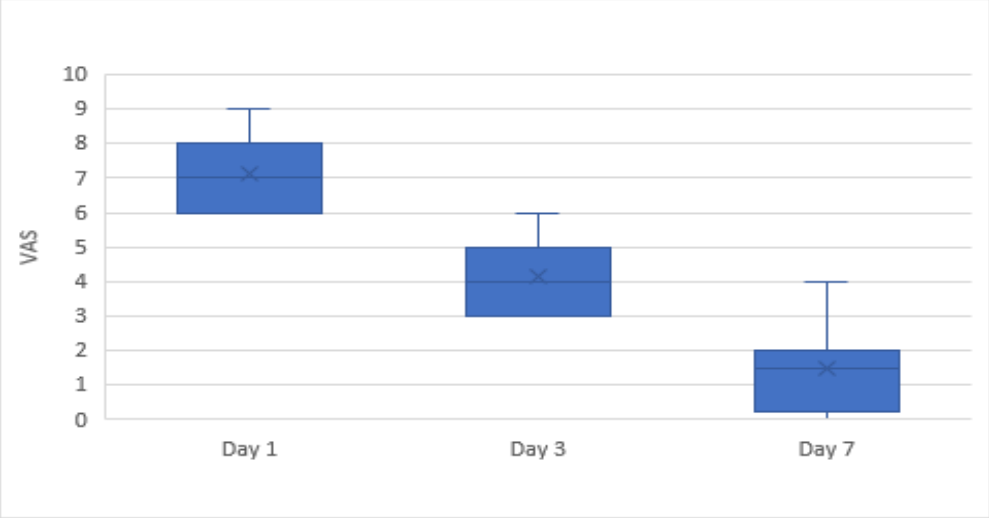

Figure 16: Box Plot showing the VAS Score

D. Accuracy of Titanium mesh

The accuracy of 3D-customized titanium mesh placement relative to the virtual mesh design was quantified and presented as mean ± SD. The mean deviation was 0.3371 ± 1.760 (units as reported in the Methods). Accuracy data are provided in Table 5 and visualized on Fig. 17.

Table 5: Accuracy of the titanium mesh placement

	Mean	SD	Median	Minimum	Maximum	Range	95.0% Lower CL for Mean	95.0% Upper CL for Mean
Accuracy of the Titanium mesh	.3371	.1760	.3086	.1220	.5676	.4456	.1899	.4842

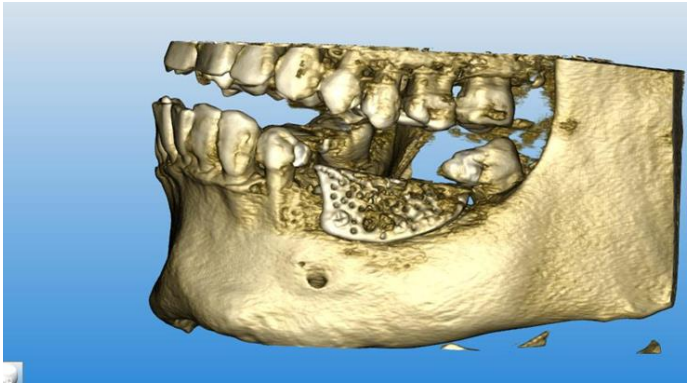

Figure 17: Image showing the superimposition of the 3D printed customized mesh after surgical placement with the virtually planned mesh (measuring the accuracy by RealGuide software)

Tianjin Daxue Xuebao (Ziran Kexue yu Gongcheng Jishu Ban)/
Journal of Tianjin University Science and Technology
ISSN (Online):0493-2137
E-Publication: Online Open Access
Vol: 59 Issue: 06:2026
DOI: 10.5281/zenodo.20606131

Summary of key findings

The applied 3D-customized titanium mesh technique produced substantial and statistically significant increases in both augmented ridge bone height and width at the assessed postoperative interval. Bone height increased by a mean of 47.1% and bone width by a mean of 155.4%, both with $p < 0.001$. Clinical outcomes were favorable: all implants remained stable with no clinical mobility or augmentation failures observed through six months, and the six-month survival rate was 100%. Early minor soft tissue complications occurred in two cases and were resolved with conservative chlorhexidine therapy; no mesh exposures were observed at six months. Patient-reported postoperative pain declined over the first week, with a statistically significant reduction by day 7. The surgical placement of the 3D-customized titanium mesh showed close agreement with the virtual plan, as reflected by the reported mean accuracy deviation. Together, these findings indicate effective hard-tissue augmentation with predictable clinical and patient-centered outcomes; detailed numerical data are reported in Table 2, Table 3, Table 5, and Figs. 16, 18, 20, and 21.

DISCUSSION

The present randomized clinical trial evaluated the clinical and radiographic efficacy of three-dimensional (3D) customized titanium mesh combined with sticky bone and simultaneous implant placement for augmenting vertically and horizontally deficient posterior mandibular alveolar ridges in 8 patients (16 implants). Overall, the technique demonstrated high efficacy, predictable bone gain, low complication rates, and excellent mesh adaptation, supporting its use for tridimensional implant site development.

Surgical and healing outcomes in this cohort were favorable, with few complications and no negative influence on bone augmentation success; bone augmentation was achieved in all cases (100% success). This result concurs with literature emphasizing the advantages of customized titanium meshes for accurate bone regeneration because of their precise fit and space-maintaining properties (Tallarico *et al.,* 2020). Although soft tissue dehiscence occurred transiently in two cases at two weeks, both were managed conservatively and resolved by the 6-month follow-up without mesh exposure. Similarly low rates of mucosal rupture have been reported by Sumida *et al.* (2015) and management strategies for exposures have been synthesized in systematic reviews (Cunha *et al.,* 2022). Conversely, higher exposure rates reported by Ciocca *et al*. (2018) and by Di Spirito *et al*. (2024) highlight that wound opening and mesh exposure remain the main complications after customized mesh procedures. Such variability likely reflects differences in surgical experience, virtual design choices (for example, leaving at least 2 mm from adjacent teeth to avoid bacterial pathways), patient-related factors, and postoperative management.

Patient-reported postoperative pain decreased significantly from Day 1 to Day 7 ($p < 0.001$), indicating rapid improvement in early postoperative discomfort and supporting realistic counseling about recovery expectations. The reduction in invasiveness and operative time attributable to preoperative virtual planning and the tailored fit of

Tianjin Daxue Xuebao (Ziran Kexue yu Gongcheng Jishu Ban)/
Journal of Tianjin University Science and Technology
ISSN (Online):0493-2137
E-Publication: Online Open Access
Vol: 59 Issue: 06:2026
DOI: 10.5281/zenodo.20606131

customized meshes may partly explain lower early morbidity, as suggested by Elboraey *et al*. (2025).

Preoperative cone-beam computed tomography (CBCT) was used to assess baseline ridge dimensions and exclude pathology. Use of CBCT improved measurement accuracy of buccal and lingual plate thickness and has been shown to correlate with primary implant stability (Al-fakeh *et al*., 2022; Isoda *et al*., 2012). Accurate preoperative imaging combined with patient-specific digital planning likely contributed to the predictable clinical outcomes observed.

Sticky bone (particulate graft combined with advanced platelet-rich fibrin) was utilized as the grafting material. Its moldability and handling advantages, plus the local release of growth factors promoting angiogenesis and bone healing, likely enhanced graft stability and integration in the dense posterior mandible (Dohan Ehrenfest *et al*., 2010; Sammartino *et al*., 2011; Simonpieri *et al*., 2016). Systematic review evidence supports sticky bone's favourable clinical and radiographic outcomes across a range of alveolar defects (Sareen *et al*., 2024).

Quantitatively, the study demonstrated highly significant increases in both alveolar ridge height (mean increase 47.1 ± 12.4%, $p < 0.001$) and width (mean increase 155.4 ± 62.1%, $p < 0.001$) at 6 months. The vertical gains align with previously reported ranges (e.g., Cucchi *et al*., 2019: 4.7–6.4 mm, 64.2 ± 22.5%), and horizontal gains are consistent with reports of clinically meaningful width augmentation using titanium mesh systems (Levine *et al*., 2022 reported mean horizontal gain 4.7 ± 1.6 mm). The notably large percentage increase in width in the present series merits cautious interpretation due to the small sample size and relative baseline dimension; nevertheless, it emphasizes the potential of customized meshes to maintain space and guide regeneration.

A critical determinant of regenerative success is mesh adaptation to the host bone. In this work, mean deviation of mesh adaptation was 0.3371 ± 0.1760 mm, indicating high fabrication and placement precision. This finding accords with reports on accurate patient-specific implant placement (Arafat *et al*., 2022), and with studies demonstrating submillimeter mean deviations for 3D-printed titanium meshes (Yang *et al*., 2022). However, larger reported deviations in other series (Chen *et al*., 2023) remind clinicians that registration and guided placement methods, including screw-position templates, may influence final accuracy and should be optimized.

Limitations of the present study include the small sample size, single-center design, and relatively short follow-up limited to 6 months post-augmentation. These factors constrain generalizability and preclude assessment of long-term implant survival and maintenance of augmented bone volume over time. Additionally, absence of a comparative control group (e.g., non-customized mesh, barrier membranes, or staged augmentation) prevents direct comparison of efficacy and complication rates.

In conclusion, within the limitations of this randomized clinical trial, 3D customized titanium mesh combined with sticky bone and simultaneous implant placement produced predictable and significant vertical and horizontal alveolar ridge augmentation in the

Tianjin Daxue Xuebao (Ziran Kexue yu Gongcheng Jishu Ban)/
Journal of Tianjin University Science and Technology
ISSN (Online):0493-2137
E-Publication: Online Open Access
Vol: 59 Issue: 06:2026
DOI: 10.5281/zenodo.20606131

posterior mandible, with low morbidity, rapid postoperative pain resolution, and submillimetric mesh adaptation accuracy. The results support the technique as an effective approach for tridimensional implant site development. Future studies with larger cohorts, longer follow-up, and comparative designs are recommended to confirm these findings, refine digital planning workflows, and identify predictors of mesh exposure and long-term volumetric stability.

CONCLUSION

Based on the observations of the current study, the following conclusions could be made:

- The use of digital workflow in construction of 3D customized titanium mesh is an effective and predictable technique for augmenting deficient posterior mandibular alveolar ridges.
- Customized titanium mesh ridge augmentation leads to significant increase in both vertical and horizontal bone dimensions.
- The 3D planned titanium mesh has high accuracy of surgical adaptation as measured by Real Guide Software.
- Future researchers should take into consideration the limitations of the present study.

References

1) Al-fakeh, H., Sharhan, H.M., Ziyad, T.A., Abdulghani, E.A., Al-Moraissi, E., Al-Sosowa, A.A., Liu, B., and Zhang, K. (2022). Three-dimensional radiographic assessment of bone changes around posterior dental implants at native bone site in Gansu Province, Northwest of China: A retrospective cohort study. *Journal of Stomatology, Oral and Maxillofacial Surgery*, 123(4), pp. e186-e191. https://doi.org/10.1016/J.JORMAS.2022.04.005

2) Arafat, S.W., Hossam Eldin, A.F., Hussien, N., Abdulmaguid, R.F., and Elbaz, M.A. (2022). The effect of Bioactive Hydrogel versus Advanced-PRF on bone regeneration following impacted mandibular third molar surgery. Clinical and CBCT Analysis. *Egyptian Dental Journal*, 68 (2), 1423-1433

3) Atwood, D.A. (1971). Reduction of residual ridges: a major oral disease entity. *J Prosthet Dent*, 26(3), pp. 266-279.

4) Cawood, J.I. and Howell, R.A. (1988). A classification of the edentulous jaws. Int J Oral Maxillofac Surg. 1988 Aug;17(4):232-6. doi: 10.1016/s0901-5027(88)80047-x.

5) Charan, J., and Biswas, T. (2013). How to Calculate Sample Size for Different Study Designs in Medical Research? *Indian J Psychol Med*, 35(2), pp. 121–126. doi: 10.4103/0253-7176.116232

6) Chen, D., Zheng, L., Wang, C., Huang, Y., Huang, H., Apicella, A., Hu, G., Wang, L., Fan, Y. (2023). Evaluation of surgical placement accuracy of customized CAD/CAM titanium mesh using screws-position-guided template: A retrospective comparative study. *Clin Implant Dent Relat Res*, 25(3), pp. 519-531. doi: 10.1111/cid.13205.

7) Chiapasco, M., Casentini, P. and Zaniboni, M. (2009). Bone augmentation procedures in implant dentistry. *Int J Oral Maxillofac Implants*, 24 Suppl, pp. 237-259. [NEW REF 7]

Tianjin Daxue Xuebao (Ziran Kexue yu Gongcheng Jishu Ban)/
Journal of Tianjin University Science and Technology
ISSN (Online):0493-2137
E-Publication: Online Open Access
Vol: 59 Issue: 06:2026
DOI: 10.5281/zenodo.20606131

8) Ciocca, L., Fantini, M., De Crescenzio, F., Corinaldesi, G. and Scotti, R. (2011). Direct metal laser sintering (DMLS) of a customized titanium mesh for prosthetically guided bone regeneration of atrophic maxillary arches. *Med Biol Eng Comput*, 49(11), pp. 1347–1352. doi: 10.1007/s11517-011-0813-4.

9) Ciocca, L., Lizio, G., Baldissara, P., Sambuco, A., Scotti, R., and Corinaldesi, G. (2018). Prosthetically CAD- CAM- guided bone augmentation of atrophic jaws using customized titanium mesh: Preliminary results of an open prospective study. *Journal of Oral Implantology*, 44(2), pp. 131–137. https://doi.org/10.1563/aaid-joi-D-17-00125

10) Cucchi, A., Chierico, A., Fontana, F., Mazzocco, F., Cinquegrana, C., Belleggia, F., Rossetti, P., Soardi, C.M., Todisco, M., Luongo, R., Signorini, L., Ronda, M. and Pistilli, R. (2019). Statements and Recommendations for Guided Bone Regeneration: Consensus Report of the Guided Bone Regeneration Symposium Held in Bologna, October 15 to 16, 2016. *Implant Dent*, 28(4), pp. 388-399. doi: 10.1097/ID.0000000000000909.

11) Cucchi, A., Bianchi, A., Calamai, P., Rinaldi, L., Mangano, F., Vingnudelli, E. and Cornaldesi, G. (2020). Clinical and Volumetric Outcomes after Vertical Ridge Augmentation using Computer-aided-design/computer-aided-manufacturing (CAD/CAM) customized titanium meshes: a pilot study. *BMC Oral Health Journal*, 20, p. 219.

12) Cunha, G., Carvalho, P.H.A., Quirino, L.C., Torres, L.H.S., Filho, VAP., Gabrielli, M.F.R. and Gabrielli, M.A.C. (2022). Titanium Mesh Exposure After Bone Grafting: Treatment Approaches-A Systematic Review. *Craniomaxillofac Trauma Reconstr*, 15(4), pp. 397-405. doi: 10.1177/19433875211046114.

13) Del Fabbro, M., Rosano, G. and Taschieri, S. (2008), Implant survival rates after maxillary sinus augmentation. European Journal of Oral Sciences, 116: 497-506. https://doi.org/10.1111/j.1600-0722.2008.00571.x

14) Di Spirito, F., Giordano, F., Di Palo, M.P., Ferraro, C., Cecere, L., Frucci, E., Caggiano, M. and Lo Giudice, R. (2024). Customized 3D-Printed Mesh, Membrane, Bone Substitute, and Dental Implant Applied to Guided Bone Regeneration in Oral Implantology: A Narrative Review. *Dent J (Basel)*, 12(10), p. 303. doi: 10.3390/dj12100303.

15) Dohan Ehrenfest, D.M., de Peppo, G.M., Doglioli, P. and Sammartino, G. (2009). Slow release of growth factors and thrombospondin-1 in Choukroun's platelet-rich fibrin (PRF): a gold standard to achieve for all surgical platelet concentrates technologies. *Growth Factors*, 27(1), pp. 63-9. doi: 10.1080/08977190802636713.

16) Dohan Ehrenfest, D.M., Del Corso, M., Diss, A., Mouhyi, J. and Charrier, J.B. (2010). Three-dimensional architecture and cell composition of a Choukroun's platelet-rich fibrin clot and membrane. *J Periodontol*, 81(4), pp. 546-55. doi: 10.1902/jop.2009.090531.

17) Elboraey, M.O., Alqutaibi, A.Y., Aboalrejal, A.N., Borzangy, S., Zafar, M.S., Al-Gabri, R., Alghauli, M.A. and Ramalingam, S. (2025). Regenerative approaches in alveolar bone augmentation for dental implant placement: Techniques, biomaterials, and clinical decision-making: A comprehensive review. *J Dent*, 154, p. 105612. doi: 10.1016/j.jdent.2025.105612.

18) Isoda, K., Ayukawa, Y., Tsukiyama, Y., Sogo, M., Matsushita, Y. and Koyano, K. (2012). Relationship between the bone density estimated by cone-beam computed tomography and the primary stability of dental implants. *Clin Oral Implants Res*, 23(7), pp. 832-6. doi: 10.1111/j.1600-0501.2011.02203.x.

19) Juodzbalys, G. and Raustia, A.M. (2004). Classification of jawbone anatomy for dental implantation. *J Oral Implantol*, 30(6), pp. 387-401. [NEW REF 11] (This is already cited in the text but listing it here as it's a cornerstone reference for the mentioned classification).

Tianjin Daxue Xuebao (Ziran Kexue yu Gongcheng Jishu Ban)/
Journal of Tianjin University Science and Technology
ISSN (Online):0493-2137
E-Publication: Online Open Access
Vol: 59 Issue: 06:2026
DOI: 10.5281/zenodo.20606131

20) Lekholm, U. and Zarb, G.A. (1985). Patient selection and preparation. In: Brånemark PI, Zarb GA, Albrektsson T, (eds.) *Tissue-Integrated Prostheses: Osseointegration in Clinical Dentistry*. Chicago, IL: Quintessence Publishing Co, pp. 199-209. [NEW REF 12] (This is the original reference for the D1-D4 bone quality classification).

21) Mateo-Sidrón Antón, M.C., Pérez-González, F. and Meniz-García, C. (2024). Titanium mesh for guided bone regeneration: a systematic review. Br J Oral Maxillofac Surg. Jun;62(5):433-440. doi: 10.1016/j.bjoms.2024.04.005.

22) Miron, R.J., Fujioka-Kobayashi, M., Hernandez, M., Kandalam, U., Zhang, Y., Ghanaati, S. and Choukroun, J. (2017). Injectable platelet rich fibrin (i-PRF): opportunities in regenerative dentistry? *Clin Oral Investig*, 21(8), pp. 2619-2627.

23) Misch, C.E. (2015). Chapter 11 – Bone Density: A Key Determinant for Treatment Planning. DOI:10.1016/B978-0-323-07845-0.00011-7

24) Otawa, N., Sumida, T., Kitagaki, H., Sasaki, K., Fujibayashi, S., Takemoto, M., Nakamura, T., Yamada, T., Mori, Y. and Matsushita, T. (2015). Custom-made titanium devices as membranes for bone augmentation in implant treatment: Modeling accuracy of titanium products constructed with selective laser melting. J Craniomaxillofac Surg. Sep;43(7):1289-95. doi: 10.1016/j.jcms.2015.05.006.

25) Raghoebar, G.M., Schoen, P., Meijer, H.J., Stellingsma, K. and Vissink, A. (2005). Mandibular fractures: a 10-year survey of treatment and complications. *J Oral Maxillofac Surg*, 63(5), pp. 655-660.

26) Sahyoun, N.R., Lin, C.L. and Krall, E. (2003). Nutritional status of the older adult is associated with dentition status. *J Am Diet Assoc*, 103(1), pp. 61-66.

27) Sammartino, G., Dohan Ehrenfest, D.M., Carile, F., Tia, M. and Bucci, P. (2011). Prevention of hemorrhagic complications after dental extractions into open heart surgery patients under anticoagulant therapy: the use of leukocyte- and platelet-rich fibrin. J Oral Implantol. Dec;37(6):681-90. doi: 10.1563/AAID-JOI-D-11-00001.

28) Sammartino, G., Dohan Ehrenfest, D.M., Shibli, J.A. and Galindo-Moreno, P. (2016).Tissue Engineering and Dental Implantology: Biomaterials, New Technologies, and Stem Cells, BioMed Research International, 5713168, https://doi.org/10.1155/2016/5713168

29) Sareen, V., Santhi, K., Saxena, I., Selvaraj, U., Vijayabharathi, V., Chauhan, S. and Gunasekaran, M. (2024). Role of Sticky Bone in the Management of Various Alveolar Bone Defects: A Systematic Review. Cureus; 16(7):e63561. doi: 10.7759/cureus.63561.

30) Tallgren, A. (1972). The continuing reduction of the residual alveolar ridges in complete denture wearers: a mixed-longitudinal study covering 25 years. *J Prosthet Dent*, 27(2), pp. 120-132.

31) Taylor, G.W., Burt, B.A., Becker, M.P., Genco, R.J., Shlossman, M., Knowler, W.C. and Pettitt, D.J. (1996). Severe periodontitis and risk for poor glycemic control in patients with non-insulin-dependent diabetes mellitus. *J Periodontol*, 67(10 Suppl), pp. 1085-1093.

32) Trisi, P. and Rao, W. (1999). Bone classification: clinical-histomorphometric comparison. *Clin Oral Implants Res*, 10(1), pp. 1-7.

33) Yang, W., Chen, D., Wang, C., Apicella, D., Apicella, A., Huang, Y., Li, L., Zheng, L., Ji, P., Wang, L. and Fan, Y. (2022). The effect of bone defect size on the 3D accuracy of alveolar bone augmentation performed with additively manufactured patient-specific titanium mesh. BMC Oral Health.;22(1):557. doi: 10.1186/s12903-022-02557-9.